The Plant Cell, Vol. 25: 134–148, January 2013, www.plantcell.org

HISTONE DEACETYLASE19 Interacts with HSL1 and Participates in the Repression of Seed Maturation Genes in *Arabidopsis* Seedlings[CW]

Yi Zhou,[a,1] Bin Tan,[a,1] Ming Luo,[b,c,1] Yin Li,[a] Chen Liu,[a] Chen Chen,[d] Chun-Wei Yu,[b] Songguang Yang,[c] Shuai Dong,[a] Jiuxiao Ruan,[a] Liangbin Yuan,[a] Zhou Zhang,[a] Linmao Zhao,[c] Chenlong Li,[d] Huhui Chen,[a] Yuhai Cui,[d] Keqiang Wu,[b,1] and Shangzhi Huang[a,1,2]

[a] State Key Laboratory of Biocontrol and Guangdong Key Laboratory of Plant Resource, School of Life Sciences, Sun Yat-Sen University, Guangzhou 510275, China

[b] Institute of Plant Biology, College of Life Science, National Taiwan University, Taipei 106, Taiwan

[c] Key Laboratory of Plant Resources Conservation and Sustainable Utilization, South China Botanical Garden, Chinese Academy of Sciences, Guangzhou 510650, China

[d] Agriculture and Agri-Food Canada, Southern Crop Protection and Food Research Centre, London, Ontario N5V 4T3, Canada

The seed maturation genes are specifically and highly expressed during late embryogenesis. In this work, yeast two-hybrid, bimolecular fluorescence complementation, and coimmunoprecipitation assays revealed that HISTONE DEACETYLASE19 (HDA19) interacted with the HIGH-LEVEL EXPRESSION OF SUGAR-INDUCIBLE GENE2-LIKE1 (HSL1), and the zinc-finger CW [conserved Cys (C) and Trp (W) residues] domain of HSL1 was responsible for the interaction. Furthermore, we found that mutations in *HDA19* resulted in the ectopic expression of seed maturation genes in seedlings, which was associated with increased levels of gene activation marks, such as Histone H3 acetylation (H3ac), Histone H4 acetylation (H4ac), and Histone H3 Lys 4 tri-methylation (H3K4me3), but decreased levels of the gene repression mark Histone H3 Lys 27 tri-methylation (H3K27me3) in the promoter and/or coding regions. In addition, elevated transcription of certain seed maturation genes was also found in the *hsl1* mutant seedlings, which was also accompanied by the enrichment of gene activation marks but decreased levels of the gene repression mark. Chromatin immunoprecipitation assays showed that HDA19 could directly bind to the chromatin of the seed maturation genes. These results suggest that HDA19 and HSL1 may act together to repress seed maturation gene expression during germination. Further genetic analyses revealed that the homozygous *hsl1 hda19* double mutants are embryonic lethal, suggesting that HDA19 and HSL1 may play a vital role during embryogenesis.

INTRODUCTION

Seed storage proteins (SSPs) play a crucial role in the life cycle of higher plants, since the amino acids produced from the degraded SSPs are used by the developing seedlings as a nutritional source during seed germination (Goldberg et al., 1994; Laux and Jurgens, 1997). The synthesis and accumulation of SSPs occur specifically during the maturation phase of seed development (Vicente-Carbajosa and Carbonero, 2005). LEAFY COTYLEDON1 (LEC1), LEAFY COTYLEDON2 (LEC2), FUSCA3 (FUS3), and ABSCISIC ACID INSENSITIVE3 (ABI3) are embryo-specific transcription factors that regulate seed maturation (Giraudat et al., 1992; Lotan et al., 1998; Luerssen et al., 1998; Stone et al., 2001). *LEC2*, *FUS3*, and *ABI3* encode related transcription factors of the B3 domain family (Giraudat et al., 1992; Luerssen et al., 1998; Stone et al., 2001). *LEC1* encodes a homolog of the subunit of CAAT box binding factors and is expressed in a seed-specific manner (Lotan et al., 1998). Mutations of *LEC1*, *LEC2*, *FUS3*, and *ABI3* genes lead to similar pleiotropic effects on the seed phenotype, including severe reduction of SSPs (Giraudat et al., 1992; Lotan et al., 1998; Luerssen et al., 1998; Harada, 2001; Stone et al., 2001; Gazzarrini et al., 2004). Conversely, ectopic expression of these genes in vegetative tissues resulted in ectopic expression of SSPs (Parcy et al., 1994; Lotan et al., 1998; Gazzarrini et al., 2004; Santos Mendoza et al., 2005; Braybrook et al., 2006). Interestingly, VP1/ABI3-LIKE (VAL) B3 proteins, VAL1/HIGH-LEVEL EXPRESSION OF SUGAR-INDUCIBLE GENE2 (HSI2) and VAL2/HSI2-LIKE1 (HSL1), act redundantly with sugar signaling to repress the ectopic expression of seed maturation genes in seedlings (Tsukagoshi et al., 2005, 2007; Suzuki et al., 2007). Both HSI2 and HSL1 contain two main domains: the plant-specific B3 domain and the zinc-finger CW (zf-CW) domain (Suzuki et al., 2007). Recently, structural and biochemical studies have identified the zf-CW domain as a member of the histone modification reader modules for epigenetic regulation (He et al., 2010). In

[1] These authors contributed equally to this work.

[2] Address correspondences to huangsz@mail.sysu.edu.cn.
The author responsible for distribution of materials integral to the findings presented in this article in accordance with the policy described in the Instructions for Authors (www.plantcell.org) is: Shangzhi Huang (huangsz@mail.sysu.edu.cn).

[C] Some figures in this article are displayed in color online but in black and white in the print edition.

[W] Online version contains Web-only data.

www.plantcell.org/cgi/doi/10.1105/tpc.112.096313

addition, HSI2 and HSL1 contain sequences similar to the EAR motif, which is a gene repression domain also found in the class II ERF transcriptional repressors and TFIIIA-type zinc-finger proteins (Ohta et al., 2001). The molecular mechanisms of how HSI2 and HSL1 are involved in the repression of the seed maturation genes in seedlings are still unclear.

Recent studies suggest that epigenetic mechanisms are involved in regulation of seed maturation genes. Histone modifications were found to be associated with ectopic expression of the *phaseolin* (*phas*) gene, a seed-specific gene in French bean (*Phaseolus vulgaris*) (Ng et al., 2006). Nucleosome loss and histone modifications were also found to regulate *oleosin* and *Ara h 3* gene expression in developing peanut (*Arachis hypogaea*) embryos (Li et al., 2009; Fu et al., 2010). PICKLE (PKL), a CHD3 chromatin remodeling factor, acts in concert with gibberellin to repress embryonic traits after germination (Ogas et al., 1997, 1999; Dean Rider et al., 2003; Henderson et al., 2004; Rider et al., 2004; Li et al., 2005). PKL is also necessary to repress *ABI3* and *ABI5* expression during germination in response to abscisic acid (Perruc et al., 2007). *Polycomb* group proteins were demonstrated to maintain a repressed state of seed gene expression by methylation of H3K27 (Köhler and Grossniklaus, 2002; Makarevich et al., 2006), and *Polycomb* group protein EMF2 was found to act synergistically with histone methylase SDG8 in repressing the embryonic program during seedling development (Tang et al., 2012a). *Arabidopsis thaliana* BRAHMA, a SNF2 chromatin-remodeling ATPase, was found to be associated with the repression of some seed maturation genes in leaves (Tang et al., 2008). ASIL1 (for *Arabidopsis* 6b-interactin protein 1-like1), a member of the plant-specific Trihelix family of DNA binding transcription factors, was found to be a negative regulator of seed maturation genes in seedlings (Gao et al., 2009). Recently, *ARGONAUTE1* was found to be involved in repressing the seed maturation genes in *Arabidopsis* seedlings, suggesting that microRNA participates in the repression of the seed maturation program during vegetative development in *Arabidopsis* (Tang et al., 2012b).

During germination, inhibition of histone deacetylase (HDAC) activity with trichostatin A, a specific inhibitor of HDACs, leads to ectopic expression of late embryonic genes in *Arabidopsis* (Tai et al., 2005). Furthermore, HDA6 and HDA19, two *Arabidopsis* HDACs, have been implicated to contribute to the repression of embryo-specific genes during germination (Tanaka et al., 2008). A double RNA interference line with both HDA6 and HDA19 knocked down displayed growth arrest after germination and the formation of embryo-like structures on the true leaves of 6-week-old plants (Tanaka et al., 2008). These observations suggest that HDA6 and HDA19 may contribute to the repression of embryonic properties after germination, but whether they directly or indirectly repress the embryo-specific genes is still unclear.

In this study, we further investigate the involvement of HDA19 in the repression of seed maturation genes. Chromatin immunoprecipitation (ChIP) assays indicate that increased expression of seed maturation genes in seedlings was correlated with histone hyperacetylation of chromatin in the *hda19* mutant. In addition, the mutation of *HSL1* resulted in elevated transcription levels of certain seed maturation genes in seedlings, which was accompanied by the change of histone acetylation and methylation. Furthermore, we show that HDA19 interacted with HSL1 both in vitro and in vivo. Our findings suggest that HDA19 and HSL1 could act together in a protein complex to repress the expression of seed maturation genes in seedlings and play a vital role in regulating the transition from seed maturation to seedling growth.

RESULTS

HDA19 Interacts with HSL1

Previous studies suggest that HSI2/VAL1 and HSL1/VAL2 are redundant inhibitors of sugar-inducible ectopic expression of seed maturation genes during seedling growth and the two proteins together play an essential role in regulating the transition from seed maturation to active seedling growth (Suzuki et al., 2007; Tsukagoshi et al., 2007). Both HSI2 and HSL1 belong to the ABI3 family and contain a plant-specific B3 DNA binding domain. In addition, HSI2 and HSL1 contain the zf-CW domain, which has been identified as a member of the histone modification reader modules for epigenetic regulation (He et al., 2010). Using the Database of Protein Domain Interactions (http://domine.utdallas.edu/cgi-bin/Domine), it is predicted that HDA19 may interact with the zinc-finger domain. We therefore tested whether there is a direct protein–protein interaction between HDA19 and HSI2 or HSL1. The yeast two-hybrid assay indicated that HDA19 interacted with HSL1 but not HSI2 (Figure 1).

To further confirm the interaction between HDA19 and HSL1, bimolecular fluorescence complementation (BiFC) and coimmunoprecipitation (Co-IP) assays were used. Previous studies have proved that HDA19 is localized in the nucleus (Zhou et al., 2005; Fong et al., 2006). The localization of HSL1 was analyzed by expressing a gene encoding an HSL1-YFP

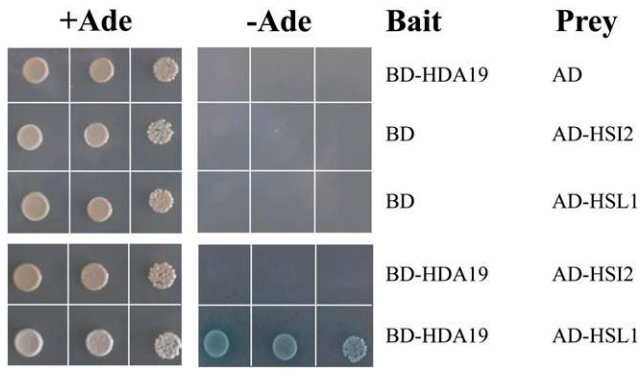

Figure 1. HDA19 Interacts with HSL1 in Yeast Two-Hybrid Assays.

Top: Test for autonomous activation of HDA19, HSI2, and HSL1. Bottom: Interaction assay with HSI2 and HSL1 as preys (fused to the AD) and HDA19 as a bait (fused to the BD). Interaction was determined by growth assay on medium lacking adenine. Dilutions (1, 10^{-1}, and 10^{-2}) of saturated cultures were spotted onto the plates.
[See online article for color version of this figure.]

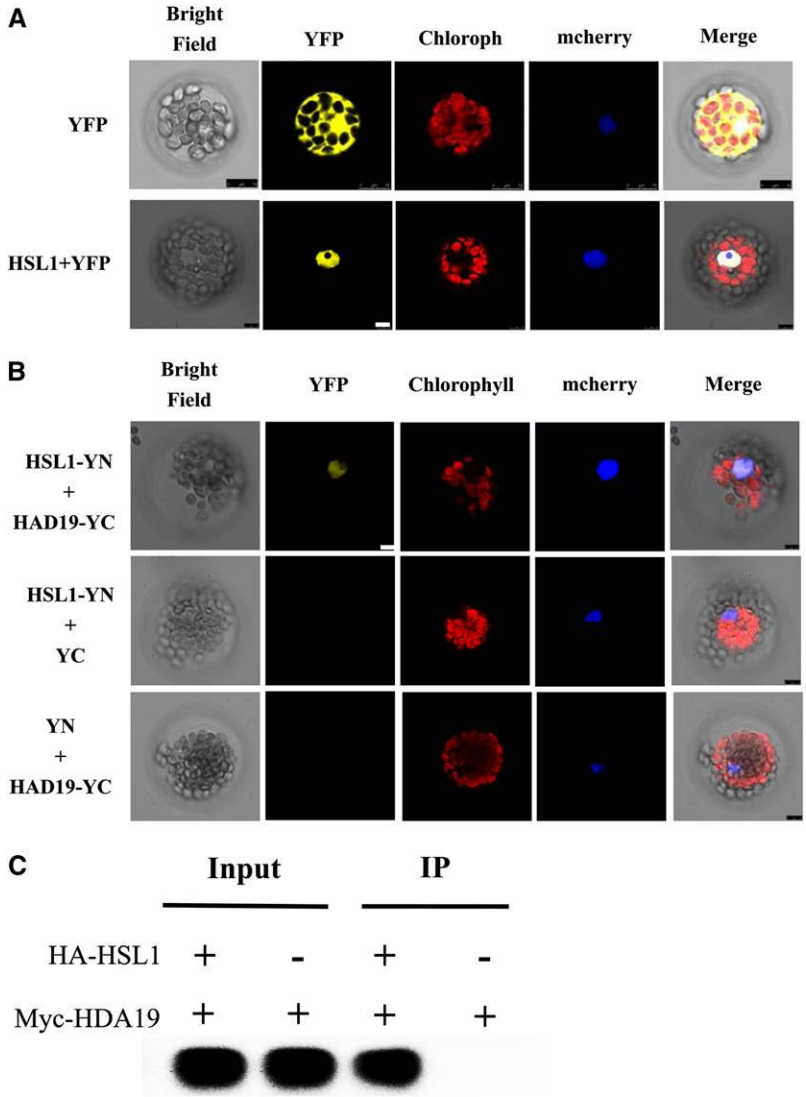

Figure 2. BiFC Visualization and Co-IP Experiments Show Interaction between HDA19 and HSL1.

(A) Subcellular localization of HSL1. Protoplasts were isolated from *Arabidopsis* seedlings. Confocal images of transgenic protoplasts ($35S_{pro}$:*YFP* and $35S_{pro}$:*HSL1-YFP*). Bars = 7.5 μm.
(B) BiFC in *Arabidopsis* protoplasts showing the interaction between HDA19 and HSL1 in living cells. HDA19 fused with the C terminus of YFP (YC) and HSL1 fused with the N terminus of YFP (YN) were cotransfected into protoplasts and visualized using confocal microscopy. As a negative control, HSL1 fused with YN and empty vector YC as well as HDA19 fused with YC and empty vector YN were cotransfected into protoplasts. Bars = 7.5 μm.
(C) Co-IP assay showing HDA19 interaction with HSL1. Tobacco leaves coexpressing 35S:HA-HSL1 and 35S:Myc-HDA19 or only 35S:Myc-HDA19 was used to immunoprecipitate with the anti-HA antibody, and the immunoblot was probed with the anti-Myc antibody.

(for yellow fluorescent protein) fusion protein under the control of the 35S promoter in the *Arabidopsis* protoplasts. As shown in Figure 2A, the HSL1-YFP fusion protein was localized in the nucleus of the *Arabidopsis* cells. The localization of HDA19 in the *hsl1* mutant was also analyzed by expressing a gene encoding an HDA19-YFP fusion protein under the control of the 35S promoter in the *hsl1-1* (SALK_059568; Tsukagoshi et al., 2007) protoplasts. The HDA19-YFP fusion protein was localized in the nucleus of the *hsl1-1* cells (see Supplemental Figure 1 online). For BiFC assays, HSL1 was fused to the N-terminal 174–amino acid protein of YFP in the pEarleyGate201 vector (pEarleyGate201-YN), and HDA19 was fused to the C-terminal 66–amino acid protein of YFP in the pEarleyGate202 vector (pEarleyGate202-YC) (Lu et al., 2010; Tian et al., 2011). The corresponding constructs were codelivered into protoplasts of *Arabidopsis*, and fluorescence was observed using a confocal microscope. As shown in Figure 2B, yellow fluorescence was clearly visible in the nucleus. Similar results were also observed using rice (*Oryza sativa*) protoplasts (see Supplemental Figure 2 online). These data indicated that HDA19 interacts

with HSL1 in the nucleus. The Co-IP assay was also performed to further determine the interaction between HDA19 and HSL1. Tobacco (*Nicotiana tabacum*) leaves were infiltrated with *Agrobacterium tumefaciens* cultures carrying 35S:HA-HSL1 and 35S:Myc-HDA19, and leaf extracts were analyzed by Co-IP. When 35S:HA-HSL1 and 35S:Myc-HDA19 fusion proteins were transiently coexpressed in tobacco leaf cells, the Myc-HDA19 fusion protein can be coimmunoprecipitated with HA-HSL1 (Figure 2C).

In order to identify the specific regions of HSL1 and HDA19 that are involved in the interaction, we generated four and three deletion constructs of *HSL1* and *HDA19*, respectively (Figure 3A). It was found that HDA19 interacted with the HSL1-ZF but not HSL1-B3, HSL1-EAR, and HSL1-ΔZF (Figure 3B, top), whereas HSL1-ZF only interacted with HDA19-UR1 (Figure 3B, bottom). BiFC and Co-IP assays further confirmed that HSL1-ZF and HDA19-UR1 are responsible for the interaction between HSL1 and HDA19 (see Supplemental Figures 3 and 4 online). These results suggest that HDA19 can directly interact with HSL1, and the zf-CW domain in the C-terminal region of HSL1 and the UR1 region of HDA19 are responsible for the interaction between these two proteins.

HDA19 and HSL1 Contribute to the Repression of Seed Maturation Genes during Seed Germination

Based on the database from The Arabidopsis Information Resource (TAIR) (http://bbc.botany.utoronto.ca/efp/cgi-bin/efpWeb.cgi), the expression of many seed maturation genes was relatively high in the later stages of embryo development (curled cotyledons and green cotyledons) but low in the early stages of embryo development (globular, heart, and torpedo) (Figure 4A). By contrast, we found that the expression of both *HDA19* and *HSL1* was higher in the early stages of embryo development (heart and

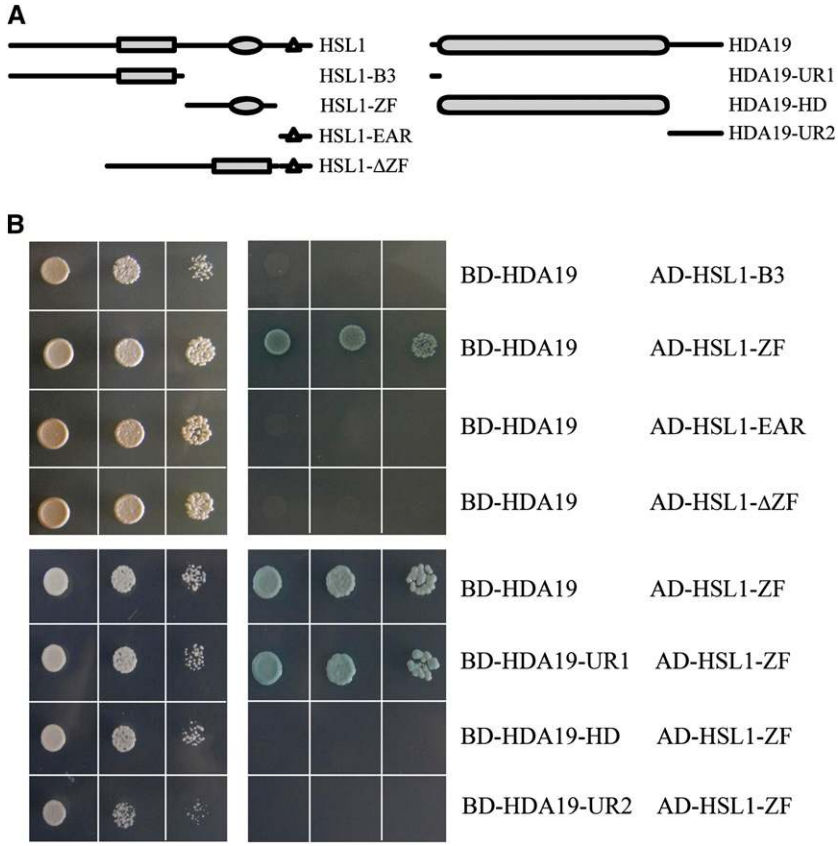

Figure 3. Different Regions Required for Interaction between HSL1 and HDA19 in Yeast Two-Hybrid Assays.

(A) Left: Diagrams of HSL1 constructs for interaction studies. Quadrate boxes represent B3 domains, elliptical boxes represent ZF domains, and triangular boxes represent EAR motifs. Right: Diagrams of HDA19 constructs for interaction studies. Rounded rectangles represent HD domains of HDA19. In the front of the HD domain is unknown region 1, designated as UR1, and at the back of the HD domain is unknown region 2, designated as UR2.

(B) Top: Interaction assay with HDA19 as a bait and different deletions of HSL1 as putative preys. Schemes of HSL1 domains and the different protein deletions are shown. Bottom: Interaction assay with the ZF domain of HSL1 as a prey and different deletions of HDA19 as putative baits. Schemes of HDA19 domains and the different protein deletions are shown. Interaction was determined by growth assays on medium lacking adenine. Dilutions (1, 10^{-1}, and 10^{-2}) of saturated cultures were spotted onto the plates.

[See online article for color version of this figure.]

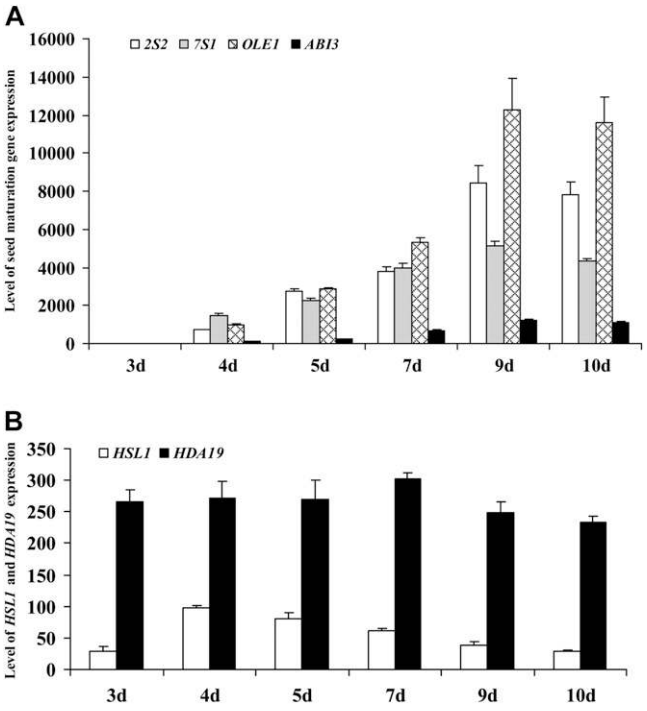

Figure 4. Gene Expression in Various Embryo Developmental Stages.

(A) Expression of seed maturation genes including *2S2*, *7S1*, *OLE1*, and *ABI3* in six stages of the embryo development (3 d, globular; 4 d, heart; 5 d, torpedo; 7 d, walking stick; 9 d, curled cotyledons; 10 d, green cotyledons). Data used for the analysis were retrieved from the database in TAIR (http://bbc.botany.utoronto.ca/efp/cgi-bin/efpWeb.cgi). The values shown are means + SD.

(B) Expression of *HSL1* and *HDA19* in six stages of embryo development (3 d, globular; 4 d, heart; 5 d, torpedo; 7 d, walking stick; 9 d, curled cotyledons; 10 d, green cotyledons). Data used for the analysis were retrieved from the database in TAIR (http://bbc.botany.utoronto.ca/efp/cgi-bin/efpWeb.cgi). The values shown are means + SD.

torpedo) than that in the later stages (curled cotyledons and green cotyledons) (Figure 4B). These expression profiling results suggest that HSL1 and HDA19 may act together to participate in regulating the transition from seed maturation to seedling growth.

The expression pattern of seed maturation genes in germinating *hda19* seedlings was analyzed by quantitative RT-PCR (qRT-PCR). We examined the expression of eight seed maturation genes, *2S2*, *7S1*, CRUCIFERINA (CRA1), OLEOSIN1 (OLE1), *LEC1*, *LEC2*, *ABI3*, and *FUS3*, in 14-d-old seedlings of a *hda19* mutant (*hda19-1*) (Tian et al., 2003). Except *FUS3*, the expression of all other genes was increased in the 14-d-old seedlings of *hda19-1* compared with Wassilewskija (Ws) wild-type seedlings (Figure 5).

The expression of the seed maturation genes, including *2S2*, *7S1*, *CRA1*, *OLE1*, *LEC1*, *LEC2*, *ABI3*, and *FUS3*, was also investigated in 14-d-old seedlings of the *hsl1-1* (Tsukagoshi et al., 2007) and *hsl1-2* mutants by qRT-PCR. Both the *hsl1-1* and *hsl1-2* mutants were in the Columbia (Col) background. As shown in Figure 6, the expression levels of *7S1*, *OLE1*, and *ABI3* were increased in the 14-d-old seedlings of *hsl1-1* and *hsl1-2* mutants compared with Col wild-type seedlings.

The Effect of the *hda19* Mutation on Histone Acetylation and Methylation during Germination

A previous study suggested that HDA19 was involved in the repression of embryo-specific genes during germination (Tanaka et al., 2008), but the underlying molecular mechanisms are unclear. To analyze whether the ectopic expression of seed maturation genes in the *hda19-1* mutant is related to the change in histone acetylation and methylation in chromatin, ChIP assays were performed to analyze the chromatin of the seed maturation genes (*2S2*, *7S1*, *CRA1*, *LEC1*, and *LEC2*) in the 14-d-old seedlings of the wild type and *hda19-1*. Since histone acetylation and methylation can occur in both the proximal promoters and/or exons (Benhamed et al., 2006; Wu et al., 2008), we therefore investigated the histone modification of the DNA sequences corresponding to the proximal promoters and the first exon regions of *2S2*, *7S1*, *CRA1*, *LEC1*, and *LEC2* (Figure 7A). As a control, we also investigated the change of histone acetylation and methylation in the proximal promoter of *ACT7* (between −690 and −557 bp) (Ng et al., 2006) in the *hda19-1* mutant seedlings compared with the Ws wild type. Since no changes in histone acetylation and methylation were found in the promoter of *ACT7* (see Supplemental Figure 5 online), we used *ACT7* as an internal control to normalize the ChIP–quantitative PCR results.

We first used antibodies specific for acetylated histone H3 and histone H4. As shown in Figures 7B and 7C increased

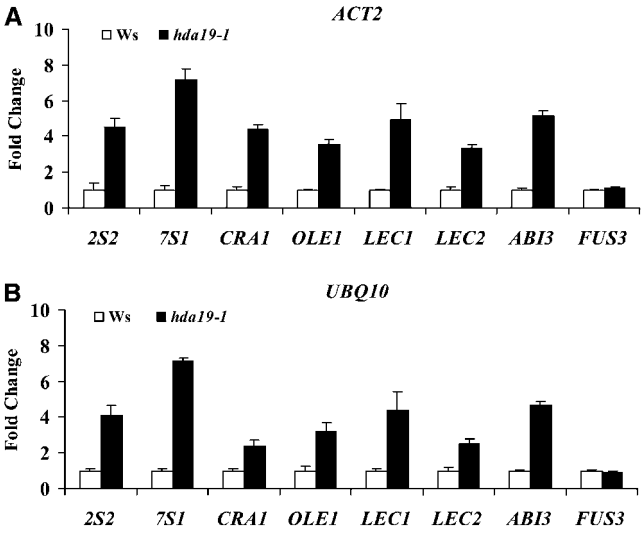

Figure 5. Expression of Seed Maturation Genes in Wild-Type (Ws) and *hda19-1* Mutant Seedlings.

The expression of *2S2*, *7S1*, *CRA1*, *OLE1*, *LEC1*, *LEC2*, *ABI3*, and *FUS3* in wild-type (Ws) and *hda19-1* seedlings grown on MS agar for 14 d was analyzed by qRT-PCR. Wild-type (Ws) RNA levels were designated as onefold. The expression values were normalized using *ACT2* **(A)** and *UBQ10* **(B)** as an internal control, respectively. Each experiment was repeated three biological replicates. Error bars represent SE.

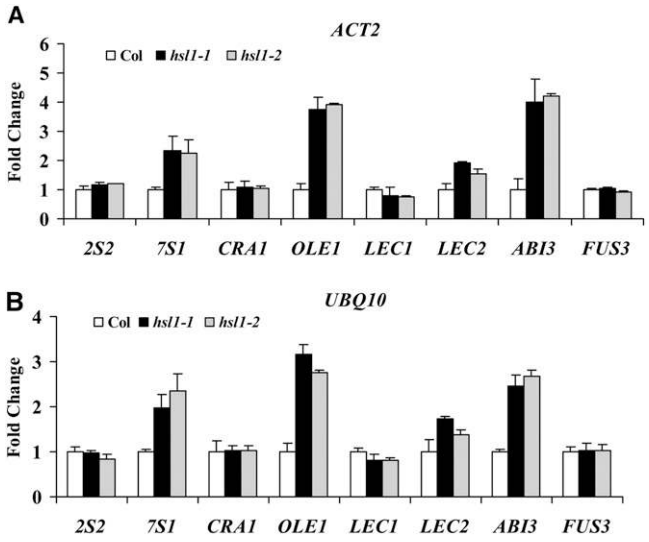

Figure 6. Expression of Seed Maturation Genes in Wild-Type (Col) and *hsl1* Mutants (*hsl1-1* and *hsl1-2*) Seedlings.

The expression of *2S2*, *7S1*, *CRA1*, *OLE1*, *LEC1*, *LEC2*, *ABI3*, and *FUS3* in wild-type (Col), *hsl1-1*, and *hsl1-2* seedlings grown on MS agar for 14 d was analyzed by qRT-PCR. Wild-type (Col) RNA levels were designated as onefold. The expression values were normalized using *ACT2* **(A)** and *UBQ10* **(B)** as an internal control, respectively. Each experiment was repeated three biological replicates. Error bars represent SE.

acetylation levels of both histones H3 and H4 in the proximal promoter (P1) and/or coding region (C1) of *2S2*, *7S1*, *CRA1*, *LEC1*, and *LEC2* were observed in the *hda19-1* seedlings. We also performed ChIP assays with antibodies specific for acetylated Lys residues of histone H3 and H4. As shown in Supplemental Figure 6 online, the increased acetylation levels of H3K9, H3K14, H4K5, and H4K12 on P1 and/or C1 regions of these genes were also observed in *hda19-1*. These results are consistent with Ng et al. (2006) that H3K9ac, H3K14ac, H4K5ac, and H4K12ac are involved in activating the expression of seed maturation genes.

ChIP analyses were also performed using antibodies specific for methylated Lys residues of H3K4, H3K27, and H3K9. ChIP using the H3K4me3 antibody showed that H3K4me3 was increased on the P1 region and/or C1 region of *2S2*, *7S1*, *CRA1*, *LEC1*, and *LEC2* in the *hda19-1* mutant (Figure 7D). This result is in line with the general observation that trimethylation at H3K4 is associated with gene activation (Strahl et al., 1999; Litt et al., 2001; Ng et al., 2003). By contrast, ChIP using H3K27me3 and H3K9me2 antibodies showed that these methylation marks were decreased on the P1 region and/or C1 region of these genes in the *hda19-1* background (Figure 7E; see Supplemental Figure 7 online). These data were consistent with the observations that H3K27me3 was required for the repression of seed maturation genes and H3K9me2 was generally associated with silenced genes (Mutskov and Felsenfeld, 2004; Bouyer et al., 2011).

We further performed ChIP-Seq analysis using the H3K14ac and H3K9me2 antibodies in the 14-d-old seedlings of Ws and *hda19-1*. In Ws, we identified 1334 genes that underwent H3K14ac acetylation (see Supplemental Data Set 1 online), but only four of them (*ASIL2* [AT3G14180], *OLE4* [AT3G27660], *CRF6* [AT3G61630], and *PXY* [AT5G61480]) were found to be involved in seed development. By contrast, we identified 3131 genes that underwent H3K14ac acetylation in *hda19-1* (see Supplemental Data Set 2 online), and 38 of them were involved in seed development (see Supplemental Data Set 3 online). We also identified 4026 and 5869 genes that underwent H3K9me2 methylation in Ws and *hda19-1*, respectively (see Supplemental Data Sets 4 and 5 online). Among those genes that underwent H3K9me2 methylation, 12 and 21 genes were involved in seed development in Ws and *hda19-1*, respectively (see Supplemental Data Sets 6 and 7 online). In *hda19* mutants, we observed a significant increase of the H3K14Ac level of target genes, including those genes involved in seed development, indicating that HDA19 plays an important role in regulating the levels of H3K14Ac and gene activities.

The Effect of the *hsl1* Mutation on Histone Acetylation and Methylation during Germination

To analyze whether the ectopic expression of *7S1*, *OLE1*, and *ABI3* in *hsl1* mutants is also related to the change of histone acetylation and methylation in the chromatin, ChIP assay was used to analyze histone acetylation and methylation levels of *7S1*, *OLE1*, *ABI3*, *CRA1*, and *LEC2* in 14-d-old seedlings of the *hsl1-1* mutant compared with the Col wild-type seedlings. For comparison, the *hda19* mutant in Col background, *hda19-2* (SALK_139445) (Kim et al., 2008; Zhou et al., 2010), was also analyzed.

As shown in Figures 8B to 8D, increased levels of H3ac, H4ac, and H3K4me3 in the proximal promoter (P1) and coding region (C1) of *7S1*, *OLE1*, and *ABI3* were observed in the 14-d-old *hsl1-1* seedlings compared with the Col wild-type seedlings. By contrast, the abundance of H3K27me3 was decreased in the 14-d-old *hsl1-1* seedlings (Figure 8E). The levels of H3ac, H4ac, H3K4me3, and H3K27me3 were not changed in both the proximal promoter (P1) and coding region (C1) of *CRA1* and *LEC2*, which is consistent with the observation that the expression levels of *CRA1* and *LEC2* exhibited little change in the *hsl1* mutants compared with the Col wild-type plants (Figure 6). These results suggested that the ectopic expression of *7S1*, *OLE1*, and *ABI3* in *hsl1* mutants was due to the change of histone acetylation and methylation levels.

HDA19 Directly Targets to Seed Maturation Genes during Seed Germination

To further investigate whether HDA19 directly targets to seed maturation genes during seed germination, *Arabidopsis* plants overexpressing HDA19-GFP (for green fluorescent protein; 35S: HDA19-GFP) (Zhou et al., 2005) were used to perform a ChIP assay (Figures 9). For the ChIP, 14-d-old seedlings were selected to investigate the enrichment of HDA19 in the promoter and/or coding region of the seed maturation genes in the HDA19-GFP plants compared with wild-type plants. qRT-PCR was used to determine the regions enriched by ChIP with an anti-GFP antibody. As shown in Figures 9B to 9F, HDA19 was recruited

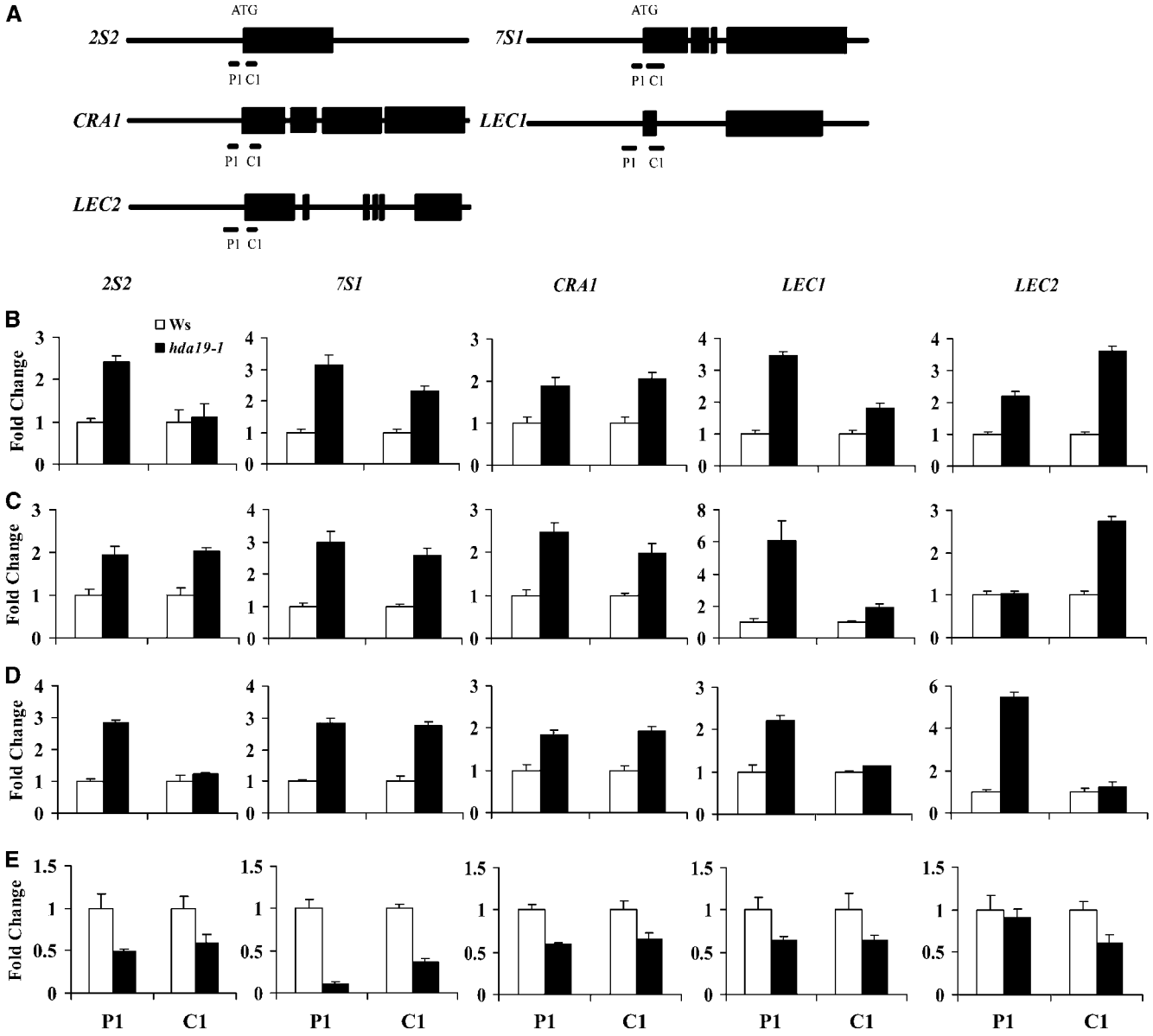

Figure 7. Levels of H3ac, H4ac, H3K4me3, and H3K27me3 in *2S2*, *7S1*, *CRA1*, *LEC1*, and *LEC2* Chromatin.

(A) Schematic structure of genomic sequences of *2S2*, *7S1*, *CRA1*, *LEC1*, and *LEC2* and the regions examined by ChIP.
(B) to **(E)** Relative levels of H3ac **(B)**, H4ac **(C)**, H3K4me3 **(D)**, and H3K27me3 **(E)** at the proximal promoter (P1) and the coding region (C1) in *2S2*, *7S1*, *CRA1*, *LEC1*, and *LEC2* in Ws wild-type and *hda19-1* seedlings grown on MS agar for 14 d. The amounts of DNA after ChIP were normalized using *ACT7* as an internal control. The value of Ws was designated as onefold. Each experiment was repeated with three biological replicates. Error bars represent SE.

to the proximal promoters (P1) of *7S1*, *LEC2*, *2S2*, *CRA1*, and *LEC1*, as well as the regions surrounding the translational starting sites (C1) of *7S1* and *LEC2* (Figures 9B and 9C), suggesting that these genes probably are direct targets regulated by HDA19.

Phenotypes of *hsl1 hda19* Double Mutants

To investigate the genetic relationship between *HSL1* and *HDA19*, we tried to generate *hsl1 hda19* double mutants. In a preliminary experiment, we failed to obtain any homozygous *hsl1 hda19* double mutants in ~300 F2 seedlings. We therefore selected one allele combination, *hsl1-1*$^{+/-}$/*hda19-2*$^{+/-}$, for detailed analysis. As shown in Figure 10A, both green round seeds and yellow wrinkled seeds were observed in the siliques from the double heterozygous plants. The embryos in the yellow wrinkled seeds were not properly developed compared with the embryos in the green round seeds (Figures 10B and 10C). We also investigated other *hsl1*$^{+/-}$/*hda19*$^{+/-}$ mutants, and similar phenotypes were observed (Table 1). Interestingly, the ratios of aborted seeds in the immature

siliques of *hsl1*$^{+/-}$/*hda19*$^{+/-}$ plants were much lower than an expected ratio of 1:16. This likely resulted from the linkage between *HSL1* and *HDA19* because both *HSL1* and *HDA19* are located on chromosome 4 (At4g32010 and At4g38130, respectively). We estimated that the recombination frequency (r) between *HSL1* and *HDA19* was ~16% and the expected ratio of total seeds to aborted seeds was ~156:1 (Meinke et al., 2009). As shown in Table 1, the actual ratio of each *hsl1*$^{+/-}$/*hda19*$^{+/-}$ plants was consistent with the expected ratio of 156:1 ($P > 0.05$).

Aborted seeds were observed in the immature and mature siliques from *hsl1*$^{-/-}$/*hda19*$^{+/-}$ and *hsl1*$^{+/-}$/*hda19*$^{-/-}$ plants (Figure 10D, Table 2). Among 300 progeny seedlings of *hsl1*$^{-/-}$/*hda19*$^{+/-}$ and *hsl1*$^{+/-}$/*hda19*$^{-/-}$ plants analyzed, no *hsl1 hda19* homozygous double mutants were obtained. Taken together, these results indicate that the homozygous *hsl1 hda19* double mutants are embryo lethal. Therefore, *HSL1* and *HDA19* may play an essential role during embryo development.

DISCUSSION

HSL1 and HDA19 Interact Physically

Similar to LEC2, FUS3, and ABI3, HSI2/VAL1 and HSL1/VAL2 also belong to the same family of B3 transcription factors

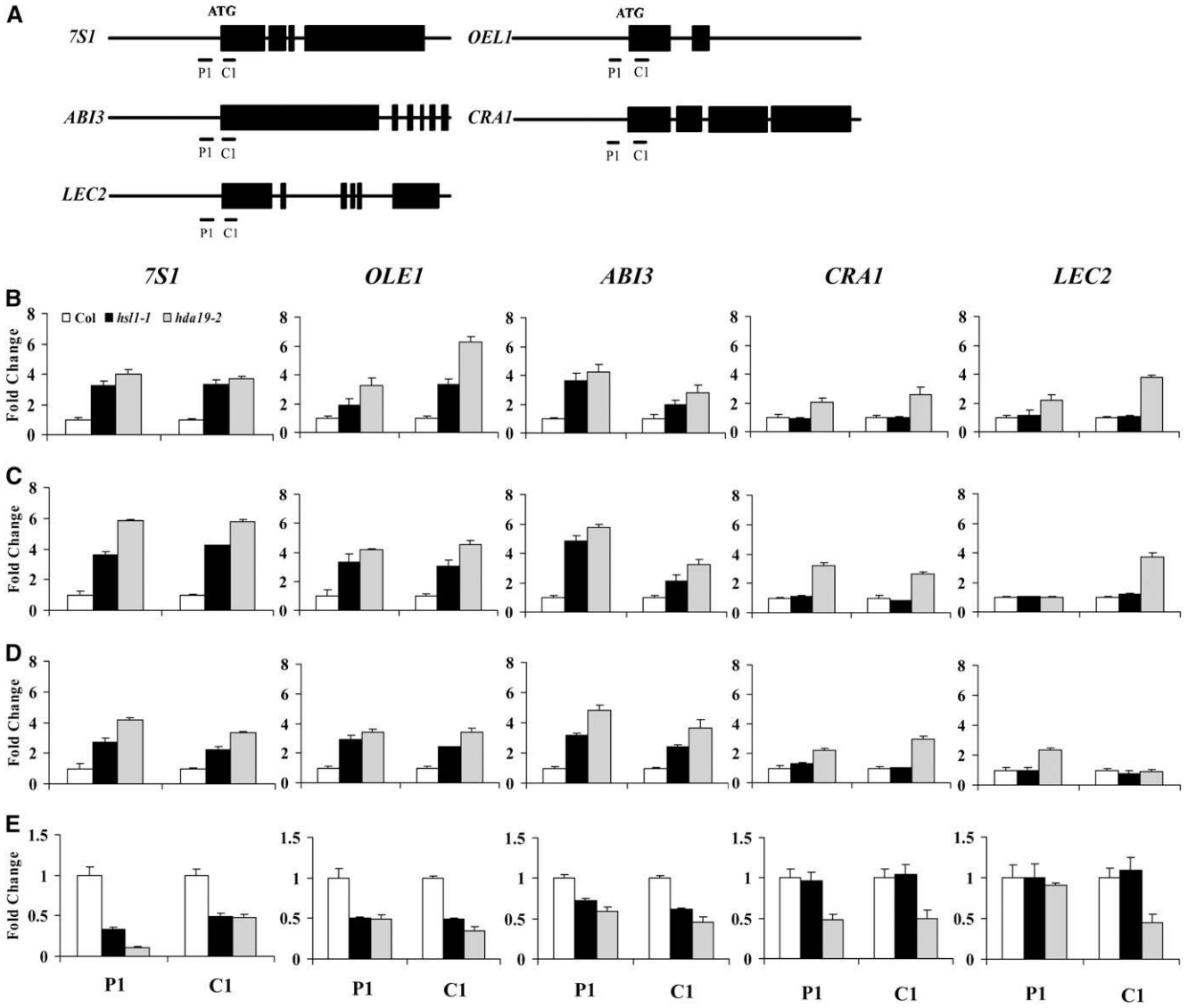

Figure 8. Levels of H3ac, H4ac, H3K4me3, and H3K27me3 in *7S1*, *OLE1*, *ABI3*, *CRA1*, and *LEC2* Chromatin.

(A) Schematic structure of genomic sequences of *7S1*, *OLE1*, *ABI3*, *CRA1*, and *LEC2* and the regions examined by ChIP.
(B) to **(E)** Relative levels of H3ac **(B)**, H4ac **(C)**, H3K4me3 **(D)**, and H3K27me3 **(E)** at the proximal promoter (P1) and the coding region (C1) in *7S1*, *OLE1*, *ABI3*, *CRA1*, and *LEC2* in wild-type (Col), *hsl1-1*, and *hda19-2* seedlings grown on MS agar for 14 d. The results were normalized for the amount of input DNA. The value of Col was arbitrarily given as 1. Each experiment was repeated three biological replicates. Error bars represent SE.

(Tsukagoshi et al., 2005). HSI2 and HSL1 act together as repressors of seed developmental programs (Suzuki et al., 2007; Tsukagoshi et al., 2007). Although monogenic mutants of the *HSI2* and *HSL1* genes are very similar to wild-type plants, *hsi2 hsl1*double mutants express a number of embryo-associated traits, including accumulation of SSPs and triacylglycerol and growth arrest after 7 to 9 d. Arrested seedlings of *hsi2 hsl1* double mutants produce embryo-like structures. Moreover, the phenotype of *hsi2 hsl1* seedlings bears a number of striking similarities to that of *pkl* seedlings, including enhanced expression of seed-associated traits upon inhibition of gibberellin biosynthesis (Suzuki et al., 2007; Tsukagoshi et al., 2007).

HDACs mediate transcriptional repression by interacting with specific DNA binding proteins or associated corepressors (Yang and Grégoire, 2005; Luo et al., 2012). Using yeast two-hybrid, BiFC, and Co-IP assays, we demonstrated that HSL1 interacts with HDA19 in the nucleus. HSI2 and HSL1 contain two main domains: the plant-specific B3 domain and the zf-CW domain (Suzuki et al., 2007). The deletion analysis of HSL1 and HDA19 proved that the zf-CW domain of HSL1 and the N-terminal UR1 region of HDA19 appeared to be required for the interaction between HDA19 and HSL1. Recent studies indicated that the zf-CW domain acts as a new histone modification reader by binding to methylated histone H3K4 (He et al., 2010; Hoppmann et al., 2011). We found that the CW domain of HSL1 recognized and interacted with HDA19, suggesting that the CW domain may have versatile functions. The tertiary structure of the zf-CW domain partially resembles that adopted by the plant homeodomain (PHD) finger bound to the histone tail, suggesting that the zf-CW domain and the PHD finger have similar functions (He

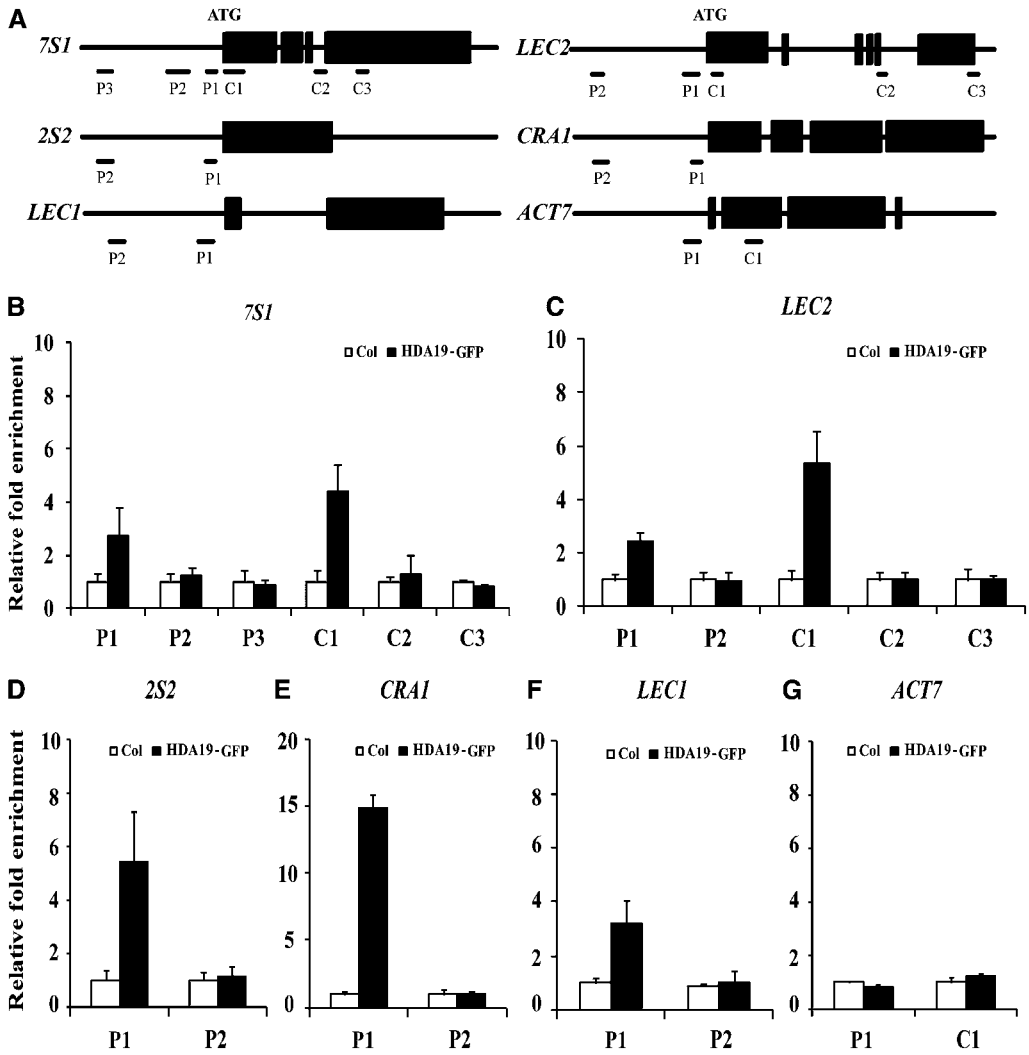

Figure 9. Target Genes of HDA19 Identified by ChIP Followed by Real-Time PCR Analysis.

(A) Schematic structure of genomic sequences of *7S1*, *LEC2*, *2S2*, *CRA1*, *LEC1*, and *ACT7* and the regions examined by ChIP.
(B) to **(G)** Transgenic plants expressing HDA19-GFP were subjected to ChIP analysis using an anti-GFP antibody. Wild-type (Col) plants were used as negative controls. *7S1* **(B)**, *LEC2* **(C)**, *2S2* **(D)**, *CRA1* **(E)**, *LEC1* **(F)**, and *ACT7* **(G)** were chosen for target genes. The results were normalized for the amount of input DNA. The value of Col was arbitrarily given as 1. Each experiment was repeated three biological replicates. Error bars represent SE.

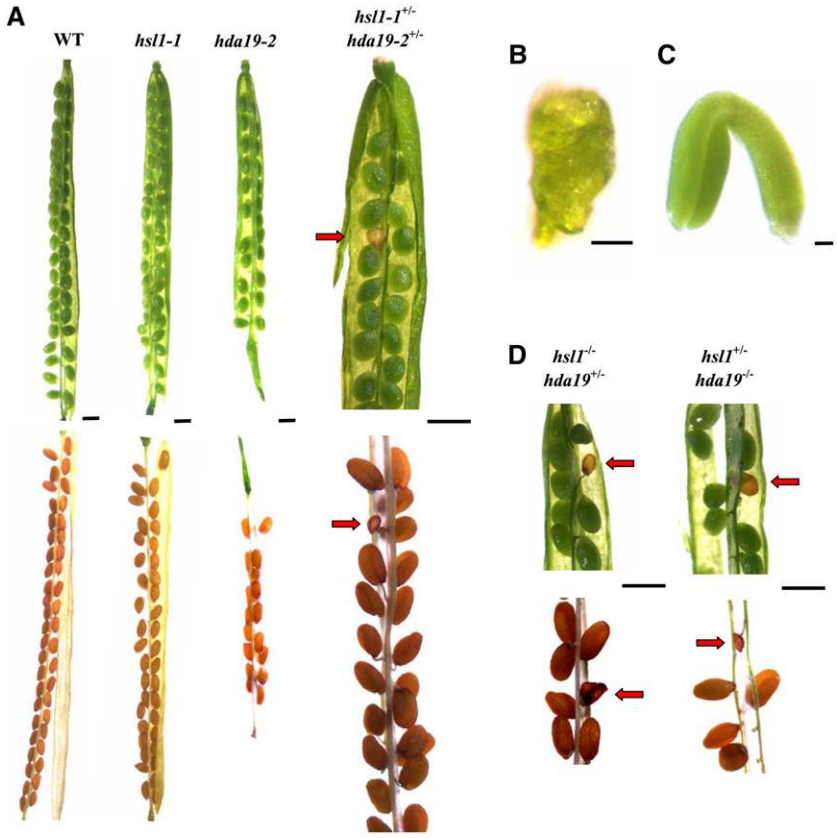

Figure 10. The Homozygous *hsl1 hda19* Double Mutant Is Seed Lethal.

(A) The dissection of immature siliques (top) and mature siliques (bottom) in *hsl1-1*$^{+/-}$/*hda19-2*$^{+/-}$ plants compared with the siliques in the wild type (WT), *hsl1-1*, and *hda19-2*. Aborted seeds are highlighted by red arrows. Bars = 500 μm.
(B) and **(C)** The phenotype of an abnormal embryo in the yellow seed **(B)** compared with the phenotype of a normal embryo in the green seed **(C)** from the same immature silique of *hsl1-1*$^{+/-}$/*hda19-2*$^{+/-}$ plant. Bars = 50 μm.
(D) The dissection of immature siliques (top) and mature siliques (bottom) in *hsl1*$^{-/-}$/*hda19*$^{+/-}$ and *hsl1*$^{+/-}$/*hda19*$^{-/-}$ plants. Aborted seeds are highlighted by red arrows. Bars = 500 μm.

et al., 2010). Some PHD fingers are able to bind histone and their nonhistone partners simultaneously by engaging different binding surfaces, mediating a direct crosstalk between the histone code readout and additional cellular pathways that those nonhistone partners participate (Li and Li, 2012). The association of a CW domain protein and a HDAC may mediate the crosstalk between histone methylation and deacetylation in gene regulation.

Two subfamilies of plant-specific B3 domain transcription factors, the AFL (for ABI3/FUS3/LEC2) B3 and VAL B3 proteins, regulate the fundamental transition between seed and vegetative phases of development (Suzuki and McCarty, 2008). The *AFL B3* genes activate the embryo maturation program, while the closely related *VAL B3* genes shut down the AFL network before germination. The functional symmetry of the *AFL* and *VAL B3* genes is mirrored in patterns of chromatin modification. The protein–protein interaction between HSL1 and HDA19 suggests that VAL B3 proteins can recruit HDACs to repress gene expression. Although no interaction between HDA19 and HSI2 was observed, it cannot be ruled out that HSI2 may interact with another HDAC.

Histone Deacetylation Mediated by HDA19 Is Required for the Repression of Seed Maturation Genes during Germination

Recent studies suggest that histone acetylation participates in the regulation of seed-specific gene expression (Tai et al., 2005; Ng et al., 2006; Tanaka et al., 2008; Li et al., 2009). We found

Table 1. Segregation Analysis of Total Seeds and Aborted Seeds in Immature Siliques of Different Genotype Heterozygous *hsl1 hda19* Double Mutants

Genotype	Total Seeds	Aborted Seeds	Ratio	P Value
hsl1-1$^{+/-}$/*hda19-2*$^{+/-}$	713	4	178.3:1	0.790
hsl1-2$^{+/-}$/*hda19-2*$^{+/-}$	1023	7	146.1:1	0.863
hsl1-1$^{+/-}$/*hda19-1*$^{+/-}$	1124	6	187.3:1	0.653
hsl1-2$^{+/-}$/*hda19-1*$^{+/-}$	1276	8	160.0:1	0.950

P value of ≥ 0.05 was considered consistent with the hypothesis of 156:1 as an expected ratio of total seeds to aborted seeds.

Table 2. Segregation Analysis of Total Seeds and Aborted Seeds in Immature Siliques of *hsl1*$^{-/-}$/*hda19*$^{+/-}$ and *hsl1*$^{+/-}$/*hda19*$^{-/-}$ Plants

Genotype	Total Seeds	Aborted Seeds	Ratio	P Value
hsl1-1$^{-/-}$/*hda19-2*$^{+/-}$	598	152	3.9:1	0.838
hsl1-2$^{-/-}$/*hda19-2*$^{+/-}$	712	195	3.7:1	0.203
hsl1-1$^{+/-}$/*hda19-2*$^{-/-}$	479	116	4.1:1	0.732
hsl1-2$^{+/-}$/*hda19-2*$^{-/-}$	293	75	3.9:1	0.838

P value of ≥ 0.05 was considered consistent with the hypothesis of 4:1 as an expected ratio of total seeds to aborted seeds.

that *hda19* mutations resulted in the ectopic expression of seed maturation genes accompanied by histone hyperacetylation, suggesting that HDA19 negatively regulates seed maturation gene transcription by reducing histone acetylation levels during germination. Histone acetylation, such as H3K9ac, H3K14ac, H4K5ac, and H4K12ac, has been linked to active gene transcription in plant cells (Kim et al., 2010; Jang et al., 2011). Ng et al. (2006) used an estradiol-inducible form of Pv ALF (an ABI3 homolog in bean) to examine the chronological changes of histone modification patterns in the promoter region of *phas*. It was found that the chromatin remodeling step induced by Pv ALF is accompanied by elevated acetylation level of H3K9 and H4K12, whereas subsequent abscisic acid–induced gene activation is accompanied by increased levels of H3K14ac and H4K5ac. We found that increased levels of seed maturation gene transcription were accompanied by the enrichment of H3K9ac, K3K14ac, H4K5ac, and H4K12ac in the *hda19-1* mutant seedlings, suggesting that the enrichment of histone acetylation plays an important role in activating stably repressed genes.

Previous studies also suggested that H3K4me3 was involved in activation of gene transcription, whereas H3K9me2 and H3K27me3 were involved in gene repression (Mutskov and Felsenfeld, 2004; Pfluger and Wagner, 2007; Zhang et al., 2007; Bouyer et al., 2011). Furthermore, elevated levels of histone acetylation were always accompanied by increased levels of H3K4me3 and reduced levels of H3K9me2 and H3K27me3 (Ng et al., 2006; Locatelli et al., 2009; Jang et al., 2011). In our study, increased levels of both histone acetylation and H3K4 trimethylation were found in the seed maturation genes of the *hda19-1* plants. In addition, increased expression of seed maturation genes was accompanied by reduced levels of gene repression marks, H3K9me2 and H3K27me3, in the *hda19-1* mutant. The genome-wide H3K14ac and H3K9me2 profiling results indicated that histone acetylation and methylation were involved in regulating the expression of seed maturation genes. Taken together, these observations suggest a synergistic interplay between histone methylation and acetylation in the regulation of gene expression.

We observed that HDA19 interacted with HSL1 though the zf-CW domain of HSL1. The zf-CW domain is a motif of ~60 residues that is frequently found in proteins involved in epigenetic regulation (Perry and Zhao, 2003). zf-CW domains have been identified in several enzymes that are involved in the control of the methylation states of the histone H3 tail, such as the *Arabidopsis* histone Lys methyltransferase SDG8 (for SET domain group 8) (Zhao et al., 2005; Wu et al., 2008; Grini et al., 2009) and the Lys-specific demethylase LSD2/KDM1B (Karytinos et al., 2009). LSD2/KDM1B is a homolog of LSD1/KDM1 that represses transcription by the demethylation of the mono- and dimethylated residue K4 in the histone H3 tail (Shi et al., 2004). In *Arabidopsis*, FLOWERING LOCUS D (FLD) encodes a plant homolog of mammalian LSD1 and is involved in the H3K4 demethylation (Jiang et al., 2007). A recent study suggested that HDA6 interacts with FLD in flowering control (Yu et al., 2011). It remains to be determined whether HDA19 can interact with other histone modification proteins, such as a histone methyltransferase or demethylase, to mediate the crosstalk between histone deacetylation and methylation/demethylation.

HSL1 Recruits HDA19 to repress the Expression of Seed Maturation Genes in Seedlings

In this study, we showed that the transcript levels of certain seed maturation genes were increased in 14-d-old *hsl1* mutant seedlings, suggesting that HSL1 is also required for the repression of seed maturation gene expression in seedlings. Furthermore, we found that the increased expression of these seed maturation genes was accompanied by the enrichment of H3ac, H4ac, and H3K4me3 and reduced levels of H3K27me3 in the *hsl1* mutant seedlings, suggesting that the repression of seed maturation genes regulated by HSL1 is involved in the change of histone modifications that may be correlated with histone deacetylation regulated by HDA19. ChIP analysis showed that HDA19 bound to the core promoters of seed maturation genes, suggesting that these genes are the direct targets of HDA19. The protein–protein interaction between HSL1 and HDA19 suggests that VAL B3 proteins, such as HSL1, may recruit a HDAC to repress gene expression. Based on these observations, we propose a model for the repression of seed maturation genes by controlling the levels of histone acetylation and methylation mediated through a protein complex containing HDA19 and HSL1.

METHODS

Plant Materials and Growth Conditions

The *Arabidopsis thaliana* wild-type Col and Ws, two *hsl1* mutants, *hsl1-1* (SALK_059568; Tsukagoshi et al., 2007) and *hsl1-2* (SALK_100053; a T-DNA insertion in the 4th exon of *HSL1*), and two *hda19* mutants, *hda19-1* (Tian et al., 2003) and *hda19-2* (SALK_139445; Kim et al., 2008; Zhou et al., 2010), were used in this study. The *hsl1-1*, *hsl1-2*, and *hda19-2* are in the Col background, whereas *hda19-1* is in the Ws background. For seed germination, sterilized seeds were incubated at 4°C for 3 d; seeds were then sown on Murashige and Skoog (MS) plates containing 1% Suc and 0.6% agar. Seedlings were grown under a 16-h-light/8-h-dark condition at 22°C in a growth room. Double mutants were obtained by genetic crosses between the single mutants and genotypes were determined by PCR (for primers, see Supplemental Table 1 online).

Yeast Two-Hybrid Assays

Yeast two-hybrid assays were performed according to the manufacturer's instructions for the Matchmaker GAL4-based two-hybrid system 3 (Clontech). The *HSI2* and *HSL1* cDNAs were subcloned into the pGADT7 vector, whereas the full-length and different deletion constructs of *HDA19*

cDNA were subcloned into the pGBKT7 vector. All constructs were transformed into yeast strain AH109 by the lithium acetate method, and yeast cells were grown on a minimal medium/-Leu-Trp according to the manufacturer's instructions (Clontech). Transformed colonies were plated onto a minimal medium/-Leu/-Trp/-His/-Ade containing 20 μg/mL 5-bromo-4-chloro-3-indolyl-α-D-galactopyranoside to test for possible interactions.

Subcellular Localization

Constructs were produced by cloning *HSL1* and *HDA19* into pEarleyGate101 (Lu et al., 2010). The resulting constructs were used for transient assays by polyethylene glycol transfection of *Arabidopsis* protoplasts (Yoo et al., 2007). Transfected cells were imaged using the TCS SP5 confocal spectral microscope imaging system (Leica).

BiFC Assays

For transfecting into *Arabidopsis* protoplasts, full-length and deleted coding sequences of *HSL1* and *HDA19* were PCR amplified and then subcloned into the pEarleyGate210-YN and pEarleyGate202-YC vectors (Lu et al., 2010; Tian et al., 2011). The resulting constructs were used for transient assays by polyethylene glycol transfection of *Arabidopsis* protoplasts (Yoo et al., 2007). For transfecting into rice (*Oryza sativa*) protoplasts, full-length coding sequences of *HDA19* and *HSL1* were PCR amplified and then subcloned into the pUC-SPYNE vector and the pUC-SPYCE vector (Walter et al., 2004), respectively. The resulting constructs were transfected into rice protoplasts as described by Bart et al. (2006). Transfected cells were imaged using the TCS SP5 confocal spectral microscope imaging system.

Co-IP Assay

To generate 35S:HA-HSL1, 35S:HA-HSL1-ZF, 35S:Myc-HDA19, and 35S:Myc-HDA19-UR1 constructs, the full-length and deletion cDNAs of *HSL1* and *HDA19* were obtained by PCR amplification and subcloned into HA-pBA and Myc-pBA vectors, respectively. Subsequently, the four constructs were introduced into *Agrobacterium tumefaciens* strain EHA105 and infiltrated into tobacco (*Nicotiana tabacum*) as described previously (Sparkes et al., 2006). Co-IP assay was performed as described (Yang et al., 2008). Two days after infiltration, tobacco leaves were harvested and ground in liquid nitrogen. Proteins were extracted in an extraction buffer (50 mM Tris-HCl, pH 7.4, 150 mM NaCl, 2 mM $MgCl_2$, 5 mM DTT, 20% glycerol, and 0.1% Nonidet P-40) containing protease inhibitor cocktail (Roche). Cell debris was pelleted by centrifugation at 13,000*g* for 12 min. The supernatant was incubated with 10 μg of anti-HA antibody or anti-Myc antibody (Clontech) at 4°C overnight. Then, 50 μL of protein A agarose beads (Clontech) was added. After 4 h of incubation at 4°C, the beads were centrifuged and washed four times with a washing buffer (50 mM Tris-HCl, pH 7.4, 150 mM NaCl, 2 mM $MgCl_2$, 5 mM DTT, 10% glycerol, and 0.1% Nonidet P-40). Proteins were eluted with 40 μL of 2.5× sample buffer and analyzed by immunoblotting using anti-Myc antibody or anti-HA antibody.

qRT-PCR Analysis

Total RNAs were extracted from seedlings using Trizol (Invitrogen) according to the manufacturer's instructions. To eliminate genomic DNA contamination, RNA was treated with DNase I (Takara) for 20 min. First-strand cDNA was synthesized from the total RNA with the Takara RNA PCR kit (Takara). qRT-PCR was performed in the IQ5 Multicolor real-time PCR detection system following the manufacturer's instructions using the SYBR Green real-time PCR master mix (Toyobo). The amount of cDNA was calculated using Bio-Rad iQ5 2.0 standard edition optical system software. qRT-PCR was conducted with three biological replicates, and each sample was conducted at least in triplicate and normalized using *ACT2* or *UBQ10* as an internal control. The primers used for qRT-PCR are listed in Supplemental Table 2 online.

ChIP Assay

The ChIP assay was performed as described (Gendrel et al., 2005). Chromatin extracts were prepared from seedlings treated by 1% formaldehyde. The chromatin was sheared to an average length of 500 bp by sonication and immunoprecipitated with specific antibodies. Antibodies used in ChIP assays were purchased from Millipore: antiacetyl-histone H3 (Millipore; 06-599), antiacetyl-histone H4 (Millipore; 06-866), antiacetyl-histone H3K9 (Millipore; 07-352), antiacetyl-histone H3K14 (Millipore; 07-353), antiacetyl-histone H4K5 (Millipore; 07-327), antiacetyl-histone H4K12 (Millipore; 07-595), antitrimethyl-histone H3K4 (Millipore; 07-473), antidimethyl-histone H3K9 (Millipore; 17-648), antitrimethyl-histone H3K27 (Millipore; 07-449), and anti-GFP (Santa Cruz Biotechnologies). ChIP assays were repeated with three biological replicates. The DNA cross-linked to immunoprecipitated proteins was analyzed by real-time qRT-PCR. Each sample was assayed in triplicate by real-time PCR. *ACT7* was used as an internal control to normalize the results. The primers used for real-time PCR analysis in ChIP assays are listed in Supplemental Table 3 online. ChIP-Seq analysis was performed as described (Lu et al., 2011).

Accession Numbers

Sequences data from this article can be found in the Arabidopsis Genome Initiative or GenBank/EMBL databases under the following accession numbers: *2S2* (At4g27150), *7S1* (At4g36700), *CRA1* (At5g44120), *OLE1* (At4g25140), *LEC1* (At1g21970), *LEC2* (At1g28300), *ABI3* (At3g24650), *FUS3* (At3g26790), *ACT2* (AT3G18780), *UBQ10* (At4g05320), *ACT7* (At5g09810), *HDA19* (At4g38130), *HSL1* (At4g32010), and *HSI2* (At2g30470).

Supplemental Data

The following materials are available in the online version of this article.

Supplemental Figure 1. Subcellular Localization of HDA19-YFP in the Protoplasts of the Wild Type (Col) and *hsl1-1* Mutants in *Arabidopsis*.

Supplemental Figure 2. BiFC in Rice Protoplasts Showing the Interaction between HDA19 and HSL1 in Living Cells.

Supplemental Figure 3. BiFC Experiments Show the Region Interaction between HDA19 and HSL1.

Supplemental Figure 4. Co-IP Experiments Show the Region Interaction between HDA19 and HSL1.

Supplemental Figure 5. Levels of H3ac, H4ac, H3K4me3, H3K27me3, H3K9ac, H3K14ac, H4K5ac, H4K12ac, and H3K9me2 in *ACT7* Chromatin.

Supplemental Figure 6. Levels of H3K9ac, H3K14ac, H4K5ac, and H4K12ac in *2S2*, *7S1*, *CRA1*, *LEC1*, and *LEC2* Chromatin.

Supplemental Figure 7. Levels of H3K9me2 in *2S2*, *7S1*, *CRA1*, *LEC1*, and *LEC2* Chromatin.

Supplemental Table 1. Primers Used for T-DNA Insertion Detection.

Supplemental Table 2. Primers Used for qRT-PCR.

Supplemental Table 3. Primers Used for ChIP Assays.

Supplemental Data Set 1. H3K14ac Occupied Chromosomal Regions in 14-d-old Ws Seedlings.

Supplemental Data Set 2. H3K14ac Occupied Chromosomal Regions in 14-d-old *hda19-1* Seedlings.

Supplemental Data Set 3. Selected Seed-Related Genes Associated with H3K14ac in 14-d-old *hda19-1* Seedlings.

Supplemental Data Set 4. H3K9me2 Occupied Chromosomal Regions in 14-d-old Ws Seedlings.

Supplemental Data Set 5. H3K9me2 Occupied Chromosomal Regions in 14-d-old *hda19-1* Seedlings.

Supplemental Data Set 6. Selected Seed-Related Genes Associated with H3K9me2 in 14-d-old Ws Seedlings.

Supplemental Data Set 7. Selected Seed-Related Genes Associated with H3K9me2 in 14-d-old *hda19-1* Seedlings.

ACKNOWLEDGMENTS

We thank Yang Zhang and Jianbin Su (Sun Yat-sen University, China) for collaboration in BiFC assays. This study was supported by Natural Science Foundation of China (31170286) and the Specialized Research Fund for the Doctoral Program of Higher Education (20100171110034) to S.H. and supported by National Science Council of Taiwan (101-2311-B-002-012-MY3 and 101-2923-B-002-005-MY3) and National Taiwan University (101R892005) to K.W. This work was also supported by National Basic Research Program of China (973 Program 2012CB910900) and the Natural Science Foundation of China (31128001).

AUTHOR CONTRIBUTIONS

S.H., K.W., and Y.Z. conceived this project and designed all research. Y.Z. and B.T. performed yeast two-hybrid research with some assistance from Y.L., C.L. and C.C. Y.Z., B.T., and M.L. performed subcellular localization and BiFC with some assistance from C.-W.Y., S.Y., L.Z., C.L., and Y.C. Y.Z. performed Co-IP assays with some assistance from B.T. and M.L. Y.Z. performed ChIP with some assistance from B.T., Y.L., C.L., C.C., S.D., J.R., L.Y., Z.Z., C.L.L., and H.C. Y.Z. performed qRT-PCR. Y.Z. performed ChIP-seq assays. Y.Z., B.T., S.D., J.R., L.Y., and Z.Z. analyzed ChIP-seq data. Y.Z. generated and analyzed *hsl1 hda19* double mutants. K.W. and Y.C. contributed BiFC, Co-IP vectors, and mutant materials. Y.Z. wrote the article. S.H., K.W., and Y.C. modified the article.

Received January 29, 2012; revised December 21, 2012; accepted December 30, 2012; published January 29, 2013.

REFERENCES

Bart, R., Chern, M., Park, C.J., Bartley, L., and Ronald, P.C. (2006). A novel system for gene silencing using siRNAs in rice leaf and stem-derived protoplasts. Plant Methods **2:** 13.

Benhamed, M., Bertrand, C., Servet, C., and Zhou, D.X. (2006). *Arabidopsis* GCN5, HD1, and TAF1/HAF2 interact to regulate histone acetylation required for light-responsive gene expression. Plant Cell **18:** 2893–2903.

Bouyer, D., Roudier, F., Heese, M., Andersen, E.D., Gey, D., Nowack, M.K., Goodrich, J., Renou, J.P., Grini, P.E., Colot, V., and Schnittger, A. (2011). Polycomb repressive complex 2 controls the embryo-to-seedling phase transition. PLoS Genet. **7:** e1002014.

Braybrook, S.A., Stone, S.L., Park, S., Bui, A.Q., Le, B.H., Fischer, R.L., Goldberg, R.B., and Harada, J.J. (2006). Genes directly regulated by LEAFY COTYLEDON2 provide insight into the control of embryo maturation and somatic embryogenesis. Proc. Natl. Acad. Sci. USA **103:** 3468–3473.

Dean Rider, S., Jr., Henderson, J.T., Jerome, R.E., Edenberg, H.J., Romero-Severson, J., and Ogas, J. (2003). Coordinate repression of regulators of embryonic identity by PICKLE during germination in *Arabidopsis*. Plant J. **35:** 33–43.

Fong, P.M., Tian, L., and Chen, Z.J. (2006). *Arabidopsis thaliana* histone deacetylase 1 (AtHD1) is localized in euchromatic regions and demonstrates histone deacetylase activity in vitro. Cell Res. **16:** 479–488.

Fu, G., Zhong, Y., Li, C., Li, Y., Lin, X., Liao, B., Tsang, E.W., Wu, K., and Huang, S. (2010). Epigenetic regulation of peanut allergen gene Ara h 3 in developing embryos. Planta **231:** 1049–1060.

Gao, M.J., Lydiate, D.J., Li, X., Lui, H., Gjetvaj, B., Hegedus, D.D., and Rozwadowski, K. (2009). Repression of seed maturation genes by a trihelix transcriptional repressor in *Arabidopsis* seedlings. Plant Cell **21:** 54–71.

Gazzarrini, S., Tsuchiya, Y., Lumba, S., Okamoto, M., and McCourt, P. (2004). The transcription factor FUSCA3 controls developmental timing in *Arabidopsis* through the hormones gibberellin and abscisic acid. Dev. Cell **7:** 373–385.

Gendrel, A.V., Lippman, Z., Martienssen, R., and Colot, V. (2005). Profiling histone modification patterns in plants using genomic tiling microarrays. Nat. Methods **2:** 213–218.

Giraudat, J., Hauge, B.M., Valon, C., Smalle, J., Parcy, F., and Goodman, H.M. (1992). Isolation of the *Arabidopsis* ABI3 gene by positional cloning. Plant Cell **4:** 1251–1261.

Goldberg, R.B., de Paiva, G., and Yadegari, R. (1994). Plant embryogenesis: Zygote to seed. Science **266:** 605–614.

Grini, P.E., Thorstensen, T., Alm, V., Vizcay-Barrena, G., Windju, S.S., Jørstad, T.S., Wilson, Z.A., and Aalen, R.B. (2009). The ASH1 HOMOLOG 2 (ASHH2) histone H3 methyltransferase is required for ovule and anther development in *Arabidopsis*. PLoS ONE **4:** e7817.

Harada, J.J. (2001). Role of *Arabidopsis* LEAFY COTYLEDON genes in seed development. J. Plant Physiol. **158:** 405–409.

He, F., et al. (2010). Structural insight into the zinc finger CW domain as a histone modification reader. Structure **18:** 1127–1139.

Henderson, J.T., Li, H.C., Rider, S.D., Mordhorst, A.P., Romero-Severson, J., Cheng, J.C., Robey, J., Sung, Z.R., de Vries, S.C., and Ogas, J. (2004). PICKLE acts throughout the plant to repress expression of embryonic traits and may play a role in gibberellin-dependent responses. Plant Physiol. **134:** 995–1005.

Hoppmann, V., Thorstensen, T., Kristiansen, P.E., Veiseth, S.V., Rahman, M.A., Finne, K., Aalen, R.B., and Aasland, R. (2011). The CW domain, a new histone recognition module in chromatin proteins. EMBO J. **30:** 1939–1952.

Jang, I.C., Chung, P.J., Hemmes, H., Jung, C., and Chua, N.H. (2011). Rapid and reversible light-mediated chromatin modifications of *Arabidopsis* phytochrome A locus. Plant Cell **23:** 459–470.

Jiang, D., Yang, W., He, Y., and Amasino, R.M. (2007). *Arabidopsis* relatives of the human lysine-specific Demethylase1 repress the expression of FWA and FLOWERING LOCUS C and thus promote the floral transition. Plant Cell **19:** 2975–2987.

Karytinos, A., Forneris, F., Profumo, A., Ciossani, G., Battaglioli, E., Binda, C., and Mattevi, A. (2009). A novel mammalian flavin-dependent histone demethylase. J. Biol. Chem. **284:** 17775–17782.

Kim, J.M., To, T.K., Nishioka, T., and Seki, M. (2010). Chromatin regulation functions in plant abiotic stress responses. Plant Cell Environ. **33:** 604–611.

Kim, K.C., Lai, Z., Fan, B., and Chen, Z. (2008). *Arabidopsis* WRKY38 and WRKY62 transcription factors interact with histone deacetylase 19 in basal defense. Plant Cell **20:** 2357–2371.

Köhler, C., and Grossniklaus, U. (2002). Epigenetic inheritance of expression states in plant development: The role of Polycomb group proteins. Curr. Opin. Cell Biol. **14:** 773–779.

Laux, T., and Jurgens, G. (1997). Embryogenesis: A new start in life. Plant Cell **9:** 989–1000.

Li, C., Wu, K., Fu, G., Li, Y., Zhong, Y., Lin, X., Zhou, Y., Tian, L., and Huang, S. (2009). Regulation of oleosin expression in developing peanut (*Arachis hypogaea* L.) embryos through nucleosome loss and histone modifications. J. Exp. Bot. **60:** 4371–4382.

Li, H.C., Chuang, K., Henderson, J.T., Rider, S.D., Jr., Bai, Y., Zhang, H., Fountain, M., Gerber, J., and Ogas, J. (2005). PICKLE acts during germination to repress expression of embryonic traits. Plant J. **44:** 1010–1022.

Li, Y., and Li, H. (2012). Many keys to push: Diversifying the 'readership' of plant homeodomain fingers. Acta Biochim. Biophys. Sin. (Shanghai) **44:** 28–39.

Litt, M.D., Simpson, M., Gaszner, M., Allis, C.D., and Felsenfeld, G. (2001). Correlation between histone lysine methylation and developmental changes at the chicken beta-globin locus. Science **293:** 2453–2455.

Locatelli, S., Piatti, P., Motto, M., and Rossi, V. (2009). Chromatin and DNA modifications in the Opaque2-mediated regulation of gene transcription during maize endosperm development. Plant Cell **21:** 1410–1427.

Lotan, T., Ohto, M., Yee, K.M., West, M.A., Lo, R., Kwong, R.W., Yamagishi, K., Fischer, R.L., Goldberg, R.B., and Harada, J.J. (1998). *Arabidopsis* LEAFY COTYLEDON1 is sufficient to induce embryo development in vegetative cells. Cell **93:** 1195–1205.

Lu, F., Cui, X., Zhang, S., Jenuwein, T., and Cao, X. (2011). *Arabidopsis* REF6 is a histone H3 lysine 27 demethylase. Nat. Genet. **43:** 715–719.

Lu, Q., Tang, X., Tian, G., Wang, F., Liu, K., Nguyen, V., Kohalmi, S.E., Keller, W.A., Tsang, E.W., Harada, J.J., Rothstein, S.J., and Cui, Y. (2010). *Arabidopsis* homolog of the yeast TREX-2 mRNA export complex: components and anchoring nucleoporin. Plant J. **61:** 259–270.

Luerssen, H., Kirik, V., Herrmann, P., and Miséra, S. (1998). FUSCA3 encodes a protein with a conserved VP1/AB13-like B3 domain which is of functional importance for the regulation of seed maturation in *Arabidopsis thaliana*. Plant J. **15:** 755–764.

Luo, M., Yu, C.W., Chen, F.F., Zhao, L., Tian, G., Liu, X., Cui, Y., Yang, J.Y., and Wu, K. (2012). Histone deacetylase HDA6 is functionally associated with AS1 in repression of KNOX genes in *Arabidopsis*. PLoS Genet. **8:** e1003114.

Makarevich, G., Leroy, O., Akinci, U., Schubert, D., Clarenz, O., Goodrich, J., Grossniklaus, U., and Köhler, C. (2006). Different Polycomb group complexes regulate common target genes in *Arabidopsis*. EMBO Rep. **7:** 947–952.

Meinke, D., Sweeney, C., and Muralla, R. (2009). Integrating the genetic and physical maps of *Arabidopsis thaliana*: Identification of mapped alleles of cloned essential (EMB) genes. PLoS ONE **4:** e7386.

Mutskov, V., and Felsenfeld, G. (2004). Silencing of transgene transcription precedes methylation of promoter DNA and histone H3 lysine 9. EMBO J. **23:** 138–149.

Ng, D.W., Chandrasekharan, M.B., and Hall, T.C. (2006). Ordered histone modifications are associated with transcriptional poising and activation of the phaseolin promoter. Plant Cell **18:** 119–132.

Ng, H.H., Dole, S., and Struhl, K. (2003). The Rtf1 component of the Paf1 transcriptional elongation complex is required for ubiquitination of histone H2B. J. Biol. Chem. **278:** 33625–33628.

Ogas, J., Cheng, J.C., Sung, Z.R., and Somerville, C. (1997). Cellular differentiation regulated by gibberellin in the *Arabidopsis thaliana* pickle mutant. Science **277:** 91–94.

Ogas, J., Kaufmann, S., Henderson, J., and Somerville, C. (1999). PICKLE is a CHD3 chromatin-remodeling factor that regulates the transition from embryonic to vegetative development in *Arabidopsis*. Proc. Natl. Acad. Sci. USA **96:** 13839–13844.

Ohta, M., Matsui, K., Hiratsu, K., Shinshi, H., and Ohme-Takagi, M. (2001). Repression domains of class II ERF transcriptional repressors share an essential motif for active repression. Plant Cell **13:** 1959–1968.

Parcy, F., Valon, C., Raynal, M., Gaubier-Comella, P., Delseny, M., and Giraudat, J. (1994). Regulation of gene expression programs during *Arabidopsis* seed development: Roles of the ABI3 locus and of endogenous abscisic acid. Plant Cell **6:** 1567–1582.

Perruc, E., Kinoshita, N., and Lopez-Molina, L. (2007). The role of chromatin-remodeling factor PKL in balancing osmotic stress responses during *Arabidopsis* seed germination. Plant J. **52:** 927–936.

Perry, J., and Zhao, Y. (2003). The CW domain, a structural module shared amongst vertebrates, vertebrate-infecting parasites and higher plants. Trends Biochem. Sci. **28:** 576–580.

Pfluger, J., and Wagner, D. (2007). Histone modifications and dynamic regulation of genome accessibility in plants. Curr. Opin. Plant Biol. **10:** 645–652.

Rider, S.D., Jr., Hemm, M.R., Hostetler, H.A., Li, H.C., Chapple, C., and Ogas, J. (2004). Metabolic profiling of the *Arabidopsis* pkl mutant reveals selective derepression of embryonic traits. Planta **219:** 489–499.

Santos Mendoza, M., Dubreucq, B., Miquel, M., Caboche, M., and Lepiniec, L. (2005). LEAFY COTYLEDON 2 activation is sufficient to trigger the accumulation of oil and seed specific mRNAs in *Arabidopsis* leaves. FEBS Lett. **579:** 4666–4670.

Shi, Y., Lan, F., Matson, C., Mulligan, P., Whetstine, J.R., Cole, P.A., Casero, R.A., and Shi, Y. (2004). Histone demethylation mediated by the nuclear amine oxidase homolog LSD1. Cell **119:** 941–953.

Sparkes, I.A., Runions, J., Kearns, A., and Hawes, C. (2006). Rapid, transient expression of fluorescent fusion proteins in tobacco plants and generation of stably transformed plants. Nat. Protoc. **1:** 2019–2025.

Stone, S.L., Kwong, L.W., Yee, K.M., Pelletier, J., Lepiniec, L., Fischer, R.L., Goldberg, R.B., and Harada, J.J. (2001). LEAFY COTYLEDON2 encodes a B3 domain transcription factor that induces embryo development. Proc. Natl. Acad. Sci. USA **98:** 11806–11811.

Strahl, B.D., Ohba, R., Cook, R.G., and Allis, C.D. (1999). Methylation of histone H3 at lysine 4 is highly conserved and correlates with transcriptionally active nuclei in Tetrahymena. Proc. Natl. Acad. Sci. USA **96:** 14967–14972.

Suzuki, M., and McCarty, D.R. (2008). Functional symmetry of the B3 network controlling seed development. Curr. Opin. Plant Biol. **11:** 548–553.

Suzuki, M., Wang, H.H., and McCarty, D.R. (2007). Repression of the LEAFY COTYLEDON 1/B3 regulatory network in plant embryo development by VP1/ABSCISIC ACID INSENSITIVE 3-LIKE B3 genes. Plant Physiol. **143:** 902–911.

Tai, H.H., Tai, G.C., and Beardmore, T. (2005). Dynamic histone acetylation of late embryonic genes during seed germination. Plant Mol. Biol. **59:** 909–925.

Tanaka, M., Kikuchi, A., and Kamada, H. (2008). The *Arabidopsis* histone deacetylases HDA6 and HDA19 contribute to the repression of embryonic properties after germination. Plant Physiol. **146:** 149–161.

Tang, X., et al. (2012b). MicroRNA-mediated repression of the seed maturation program during vegetative development in *Arabidopsis*. PLoS Genet. **8:** e1003091.

Tang, X., Hou, A., Babu, M., Nguyen, V., Hurtado, L., Lu, Q., Reyes, J.C., Wang, A., Keller, W.A., Harada, J.J., Tsang, E.W., and Cui,

Y. (2008). The *Arabidopsis* BRAHMA chromatin-remodeling ATPase is involved in repression of seed maturation genes in leaves. Plant Physiol. **147:** 1143–1157.

Tang, X., Lim, M.H., Pelletier, J., Tang, M., Nguyen, V., Keller, W.A., Tsang, E.W., Wang, A., Rothstein, S.J., Harada, J.J., and Cui, Y. (2012a). Synergistic repression of the embryonic programme by SET DOMAIN GROUP 8 and EMBRYONIC FLOWER 2 in *Arabidopsis* seedlings. J. Exp. Bot. **63:** 1391–1404.

Tian, G., Lu, Q., Zhang, L., Kohalmi, S.E., and Cui, Y. (2011). Detection of protein interactions in plant using a gateway compatible bimolecular fluorescence complementation (BiFC) system. J. Vis. Exp. **55:** 3473.

Tian, L., Wang, J., Fong, M.P., Chen, M., Cao, H., Gelvin, S.B., and Chen, Z.J. (2003). Genetic control of developmental changes induced by disruption of *Arabidopsis* histone deacetylase 1 (AtHD1) expression. Genetics **165:** 399–409.

Tsukagoshi, H., Morikami, A., and Nakamura, K. (2007). Two B3 domain transcriptional repressors prevent sugar-inducible expression of seed maturation genes in *Arabidopsis* seedlings. Proc. Natl. Acad. Sci. USA **104:** 2543–2547.

Tsukagoshi, H., Saijo, T., Shibata, D., Morikami, A., and Nakamura, K. (2005). Analysis of a sugar response mutant of *Arabidopsis* identified a novel B3 domain protein that functions as an active transcriptional repressor. Plant Physiol. **138:** 675–685.

Vicente-Carbajosa, J., and Carbonero, P. (2005). Seed maturation: Developing an intrusive phase to accomplish a quiescent state. Int. J. Dev. Biol. **49:** 645–651.

Walter, M., Chaban, C., Schütze, K., Batistic, O., Weckermann, K., Näke, C., Blazevic, D., Grefen, C., Schumacher, K., Oecking, C., Harter, K., and Kudla, J. (2004). Visualization of protein interactions in living plant cells using bimolecular fluorescence complementation. Plant J. **40:** 428–438.

Wu, K., Zhang, L., Zhou, C., Yu, C.W., and Chaikam, V. (2008). HDA6 is required for jasmonate response, senescence and flowering in *Arabidopsis*. J. Exp. Bot. **59:** 225–234.

Yang, J.Y., Iwasaki, M., Machida, C., Machida, Y., Zhou, X., and Chua, N.H. (2008). betaC1, the pathogenicity factor of TYLCCNV, interacts with AS1 to alter leaf development and suppress selective jasmonic acid responses. Genes Dev. **22:** 2564–2577.

Yang, X.J., and Grégoire, S. (2005). Class II histone deacetylases: from sequence to function, regulation, and clinical implication. Mol. Cell. Biol. **25:** 2873–2884.

Yoo, S.D., Cho, Y.H., and Sheen, J. (2007). *Arabidopsis* mesophyll protoplasts: a versatile cell system for transient gene expression analysis. Nat. Protoc. **2:** 1565–1572.

Yu, C.W., Liu, X., Luo, M., Chen, C., Lin, X., Tian, G., Lu, Q., Cui, Y., and Wu, K. (2011). HISTONE DEACETYLASE6 interacts with FLOWERING LOCUS D and regulates flowering in *Arabidopsis*. Plant Physiol. **156:** 173–184.

Zhang, X., Clarenz, O., Cokus, S., Bernatavichute, Y.V., Pellegrini, M., Goodrich, J., and Jacobsen, S.E. (2007). Whole-genome analysis of histone H3 lysine 27 trimethylation in *Arabidopsis*. PLoS Biol. **5:** e129.

Zhao, Z., Yu, Y., Meyer, D., Wu, C., and Shen, W.H. (2005). Prevention of early flowering by expression of FLOWERING LOCUS C requires methylation of histone H3 K36. Nat. Cell Biol. **7:** 1256–1260.

Zhou, C., Zhang, L., Duan, J., Miki, B., and Wu, K. (2005). HISTONE DEACETYLASE19 is involved in jasmonic acid and ethylene signaling of pathogen response in *Arabidopsis*. Plant Cell **17:** 1196–1204.

Zhou, J., Wang, X., He, K., Charron, J.B., Elling, A.A., and Deng, X.W. (2010). Genome-wide profiling of histone H3 lysine 9 acetylation and dimethylation in *Arabidopsis* reveals correlation between multiple histone marks and gene expression. Plant Mol. Biol. **72:** 585–595.